

Received: 2018.05.22
Accepted: 2018.07.04
Published: 2018.12.12

Involvement of Activation of Mitogen-Activated Protein Kinase (MAPK)/Extracellular Signal-Regulated Kinase (ERK) Signaling Pathway in Proliferation of Urethral Plate Fibroblasts in Finasteride-Induced Rat Hypospadias

Authors' Contribution:

Study Design A
Data Collection B
Statistical Analysis C
Data Interpretation D
Manuscript Preparation E
Literature Search F
Funds Collection G

ABEF **Nini An***
BC **Jinpu Peng***
BC **Guoqing He**
BC **Xia Fan**
CD **Fei Li**
AEG **Hui Chen**

Department of Pediatric Surgery, Guizhou Provincial People's Hospital, Guiyang, Guizhou, P.R. China

* Equal contribution

Corresponding Author: Hui Chen, e-mail: chenhuidpa198406@sina.com

Source of support: This project was funded by the Joint Fund of Guizhou Provincial Department of Science and Technology (LH[2016]7177)

Background: We investigated the role of the mitogen-activated protein kinase (MAPK)/extracellular signal-regulated kinase (ERK) signaling pathway in finasteride-induced hypospadias rats and explored the mechanisms involved.

Material/Methods: The hypospadias model was established by intragastric administration of finasteride and confirmed by hematoxylin and eosin (HE) staining. The urethral plate fibroblasts (UPF) were obtained from normal and modeled rats and identified based upon vimentin expression. Thereafter, UPF were divided into a normal control group, a model group, a model + MAPK inhibitor group, and a model + ERK inhibitor group. Cell proliferation, apoptosis, and cell cycling of UPF were assessed. Quantitative real-time PCR and Western blot analysis were used to evaluate expression of the MAPK signaling pathway and apoptosis-related genes.

Results: HE staining confirmed that 10 mg/kg finasteride caused severe hypospadias in rats. UPFs obtained from the 10 mg/kg finasteride group showed higher proliferation and cell cycling and lower apoptosis compared with those obtained from the normal control group ($P < 0.05$). Interestingly, a MAPK inhibitor or an ERK inhibitor could attenuate the abnormalities of cell proliferation, cycling, and apoptosis of UPF induced by finasteride. Compared with controls, the relative expression of p-MEK1/MEK1, caspase 3, and P53 in the UPF of the model group were reduced, while the relative expression of p-MAPK14/MAPK14 was increased in the cells of the model group. By contrast, a MAPK inhibitor or an ERK inhibitor could alleviate the abnormalities of MAPK/ERK signaling pathway and apoptosis-related gene expression induced by finasteride.

Conclusions: Our study reveals that the MAPK/ERK signaling pathway is involved in the regulation of proliferation, apoptosis, and cell cycling of UPFs in finasteride-induced hypospadias.

MeSH Keywords: **Finasteride • MAP Kinase Kinase Kinases • Urethral Neoplasms**

Full-text PDF: <https://www.medscimonit.com/abstract/index/idArt/911271>

 2812

 2

 6

 34



Background

Hypospadias is a common congenital malformation of the genitourinary system in children, characterized by abnormal distribution of urethral orifice and circumcision [1]. The etiology of hypospadias is unclear [2,3], but the biological activity of urethral plate fibroblasts (UPF) is typically affected [4,5]. Finasteride is a 4-nitrogen steroid hormone compound commonly used in treatment of benign prostatic hyperplasia [6]. 5- α reductase is an enzyme necessary for the conversion of testosterone to 5 α -dihydrotestosterone (DHT), while finasteride belongs to type II 5- α reductase inhibitor, which can block the transformation of testosterone to DHT and finally influence the DHT level [7]. Finasteride can affect the development of genital organs [8]. Finasteride administered to pregnant rats develop malformation of the urinary system, with hypospadias in male embryos [9]. However, its mechanisms are still largely unknown.

The mitogen-activated protein kinase (MAPK) signaling pathway is a serine/threonine protein kinase pathway through which eukaryotic cells transduce extracellular signals into the cytoplasm [10]. The MAPK signaling pathway was found to be abundant in the signal transduction pathway in hypospadias, based on whole-genome chip analysis [10]. Lai et al. found that activation of the MAPK pathway stimulated steroid production, proving that the MAPK pathway is involved in secretion of sex hormones [11]. Extracellular signal-regulated kinase (ERK) is an important member of the MAPK signaling pathway. Through phosphorylating its substrates, ERK takes part in the regulation of cell proliferation, stress, differentiation, apoptosis, and inflammation [12,13]. Abnormalities of the ERK pathway can lead to neurological and developmental diseases. However, the relationship between urinary genitalia development and the ERK signaling pathway is still unclear [14–16].

Besides their actions as structural components, fibroblasts also play a critical role in immune response to tissue injury. The uncontrolled proliferation and a huge release of growth factor from fibroblasts can induce pathological changes [17,18]. In this study, we established hypospadias in rats using finasteride and investigated the relationship between proliferation of UPFs and the MAPK/ERK signaling pathway. This study aimed to provide an experimental basis for clarifying the mechanisms involved in the occurrence and development of hypospadias.

Material and Methods

Animals and model

We obtained 20 female SD rats and 20 male rats (SPF grade, weight: ~150 g) from the Experimental Animal Center of

Nantong University. All experimental procedures were approved by the Ethics Committee of Guizhou Provincial People's Hospital (2016195). After 1 week of adaptation, a female rat and a male rat were placed in a metabolic cage. In the morning, a suppository in the metabolic cage was observed to determine conception. The female rats with a suppository were put together, and the day was marked as day 0 of pregnancy. We randomly divided 20 pregnant rats into 4 groups: a normal control group, a 10 mg/kg finasteride group, a 50 mg/kg finasteride group, and a 100 mg/kg finasteride group. Finasteride tablets (MSD International GmbH LLC) were administered intragastrically to rats on the 8th day to the 16th day according to the corresponding doses to establish hypospadias as previously described [19]. On the 18th day, the rats were killed and dissected.

The pregnant rats were weighed and anesthetized with isoflurane. Thereafter, abdominal hair was shaved and pregnant rats were fixed on the operating table and disinfected with iodophor. The abdomen was opened using surgical scissors, the whole uterus was gently exposed and was cut off with the placenta on a clean table. The amniotic membrane was opened with a carefully disinfected apparatus; the fetal rats were taken out gently and the umbilical cord was cut gently. The anal genitals distance (AGD) was measured, and testicles and penis were obtained under a stereoscopic microscope.

Hematoxylin Eosin (HE) staining

The urethral tissues were rinsed for several hours, then dehydrated, embedded, and sliced. The paraffin sections were dewaxed and hydrated. The sections were stained with HE solution for 3 min and images were taken by light microscopy.

Preparation of urethral plate fibroblasts

In the aseptic condition, urethral tissue of the fetal rats was taken out from the control and the modeled rats (10 mg/kg finasteride), and the tissues were washed with PBS 5 times. A sterile surgical scalpel was used to scrape the tissue around the urethra and then we cut the tissue into 2 mm x 2 mm pieces using ophthalmic scissors. The tissue was cultivated by direct adherent culture methods to culture fibroblasts *in vitro* in a 37°C CO₂ incubator for 4 h. After full adherence, 5 mL of Dulbecco's modified Eagle's medium containing 10% fetal bovine serum was added into the culture bottle and the medium was refreshed every 3 day. When the cell confluence reached 80%, the tissues were removed and the cells were digested by 0.25% trypsin.

The mounted cells were washed with PBS 3 times and fixed in 4% polyformaldehyde for 15 min at room temperature, blocked in 5% BSA (Solarbio) at room temperature for 30 min, and then

incubated with anti-vimentin antibody (CST) at 4°C overnight. After washing in PBS, the cells were incubated with Alexa Fluor 593 goat anti-rabbit IgG (1: 200, Life Technologies, Carlsbad, CA, USA) for 30 min at room temperature. Images were taken under fluorescence microscopy (BX51, Olympus, Japan). DAPI was used to stain the nuclei.

UPFs were divided into 4 groups: a normal control group, a model group, a model + MAPK inhibitor group, and a model + ERK inhibitor group. Equal numbers of UPFs (2×10^4 /mL) were placed on 96-well plates. After cell confluence attained 80%, serum-free medium was used to synchronize the cells for 24 h. After treatment with MAPK inhibitor or ERK inhibitor for 24 h, cell viability, apoptosis, cell cycle distribution, and protein expression were assessed.

Cell counting kit assay

After treatment with MAPK inhibitor (SB203580, 0.5 μ M) (Tocris) or ERK inhibitor (SCH772984, 4 nM) (Tocris) for 24 h, 10 μ L medium with the Cell Counting Kit (CCK)-8 (Gibco) was added into each well. After an additional 4-h incubation in a CO₂ incubator at 37°C, the absorbance was detected by a microplate reader (Thermo Fisher Scientific) at 490 nm. Cell viability was defined by optical density (OD) values.

Flow cytometry

After treatment with MAPK inhibitor or ERK inhibitor for 24 h, 5×10^5 cells were collected for Annexin V-fluorescein isothiocyanate/propidium iodide (PI) staining (cat. no. 70-AP101-100; MultiSciences, Hangzhou, China) and the proportion of apoptotic cells was detected within 1 h using a FACSCalibur flow cytometer (NovoCyte™, ACEA Biosciences) (Ex=488 nm; Em=530 nm) and data were analyzed using CellQuest Pro 5.1 (BD Biosciences, Franklin Lakes, NJ, USA). For cell cycle analysis, the cells were collected for PI staining (cat. no. 70-CCS013; MultiSciences, Hangzhou, China) for 30 min at room temperature. The Cell Cycle platform in FlowJo 10 software was used to analyze the cell cycle distribution.

Quantitative real-time PCR (QRT-PCR)

After treatment with MAPK inhibitor or ERK inhibitor for 24 h, 5×10^5 cells were obtained for QRT-PCR. mRNA was extracted using a TRIzol reagent kit (Invitrogen). Subsequently, total mRNA was transcribed into cDNA using reverse transcription kits according to the manufacturer's instructions (Takara Biotechnology Co., Dalian, China). Fluorescence QRT-PCR was utilized to detect expression levels of the targeted genes using cDNA as a template following treatment with DNA polymerase (catalog no. EP0041; Thermo Fisher Scientific) as follows: denaturation at 95°C for 45 s, annealing at 60°C for

Table 1. The primer sequences.

Genes	Primers (5'-3')
Caspase 3-F	AAAGCCGAAACTCTTCATCA
Caspase 3-R	GTCTCAATACCGCAGTCCAG
P53-F	CTCCCCAACATCTTATCCG
P53-R	ACAGGCACAAACACGAACC
GAPDH-F	GCAAGTTCAACGGCACAG
GAPDH-R	CGCCAGTAGACTCCACGAC

45 s, and extension at 72°C for 60 s for 36 cycles. The target gene expression was normalized to GAPDH. The primers were synthesized by Shanghai Sangon (Shanghai, China) (Table 1).

Western blot analysis

The cells were treated with MAPK or ERK inhibitor for 24 h and 5×10^5 cells were collected for Western blot analysis. Protein (20 μ g) was extracted from the treated cells, run on sodium-dodecyl sulfate-polyacrylamide gels (10%), and transferred to nitrocellulose membranes. The membranes were blocked by 5% non-fat milk for 2 h at room temperature. The following primary antibodies were used for overnight incubation at 4°C: anti-caspase-3 (1: 1000, bs-0081R, Bioss, Beijing, China), anti-P53 (1: 2000, Cell Signaling), anti-p-MAPK14 (1: 1000, bs-5476R, Bioss, Beijing, China), anti-MAPK14 (1: 1000, bs-28027R, Bioss, Beijing, China), anti-MEK1 (1: 1000, ABclonal), and anti-p-MEK1 (1: 1000, ABclonal). After washing, the membranes were incubated with the secondary antibody (1: 100, ab131368, Abcam) for 2 h at room temperature. An Enhanced Chemiluminescence kit (No. RPN2133; GE Healthcare Life Sciences, Chicago, IL, USA) was added to the membrane prior to visualization with a gel imaging system (Thermo Fisher Scientific).

Statistical analysis

The data were expressed as mean and standard deviation (SD). Statistical significance was calculated by one-way analysis of variance (ANOVA) with Newman-Keuls as the post hoc test (SPSS 17.0, IBM, Armonk, NY, USA). Parametric variables were described using frequency statistics and analyzed by the chi-squared test (χ^2). $P < 0.05$ was considered statistically significant.

Results

Finasteride caused hypospadias in male fetal rats

Compared with the normal control group, the anal genitals distance (AGD) in the finasteride groups was shortened (Table 2), and the difference between finasteride (10 mg/kg or 50 mg/kg)

Table 2. Finasteride caused hypospadias in male fetal rats.

	Control	Finasteride		
		10 mg/kg	50 mg/kg	100 mg/kg
No. of pregnant rats (N)	5	5	5	5
No. of male fetal	12	10	7	5
AGD in male fetal (mm)	1.89±0.73	1.54±0.13*	1.38±0.21*	1.88±0.26
Weight (g)	1.38±0.29	1.50±0.12	1.35±0.09	1.5±0.07
No. of male embryos with hypospadias	0	3*	4*	3*
Rate of hypospadias	0	30%*	57%*	60%*

Compared with control, * P<0.05.

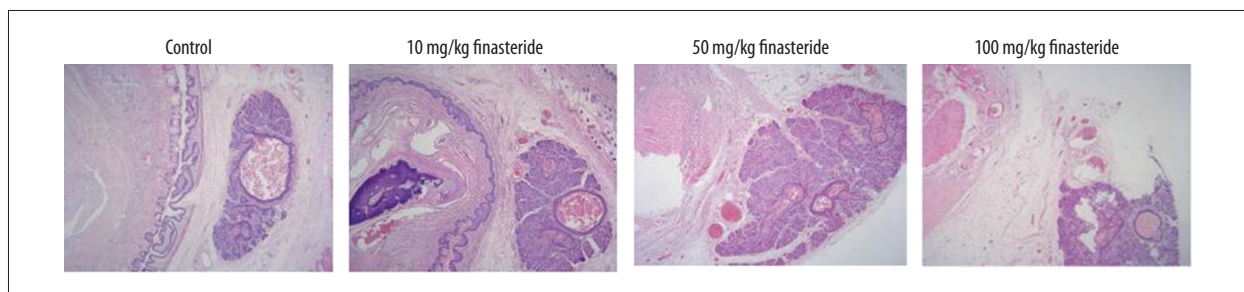


Figure 1. Morphological changes shown by HE staining. Magnification: 200×.

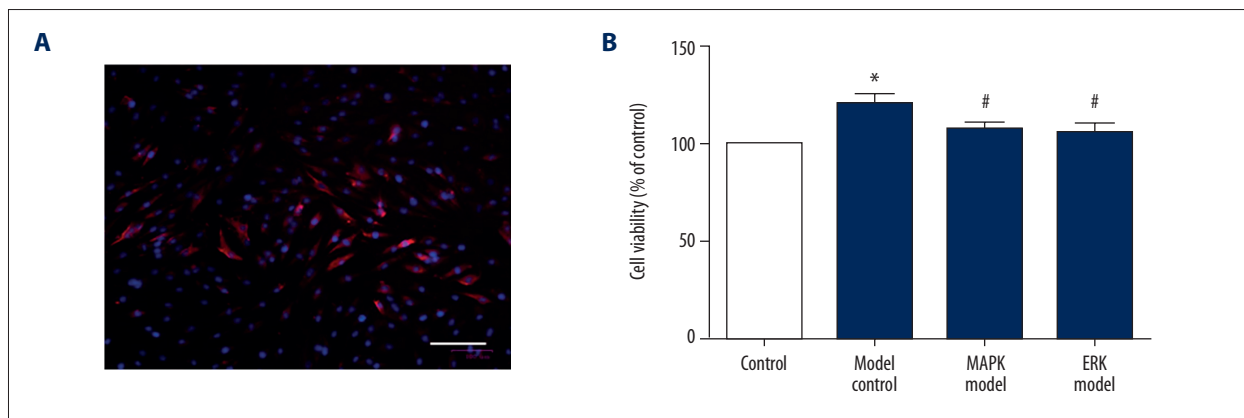


Figure 2. Proliferation of urethral plate fibroblasts was attenuated by MAPK inhibitor or ERK inhibitor. (A) Identification of urethral plate fibroblasts by immunofluorescence. Scale bar: 100 µm; (B) CCK-8 assay of cell viability. Compared with control, * P<0.05; compared with model, # P<0.05.

group and control group was statistically significant (P<0.05). The numbers of male rats and weight of the rats in each group were comparable. The numbers of hypospadias rats were significantly elevated in finasteride groups (10 mg/kg, 50 mg/kg, 100 mg/kg) compared with control (P<0.05). The rate of hypospadias was significantly increased in finasteride-treated groups (10 mg/kg, 50 mg/kg, 100 mg/kg) compared with control (P<0.05).

HE staining showed that the size of the cavernous sinus of the normal control group was relatively uniform, and the tissue layers between the white membrane and skin were abundant and loose (Figure 1). Rats in the finasteride groups showed more penile dysplasia in comparison with the normal control group, among which the 10 mg/kg finasteride group showed the most serious abnormality. Rats in the finasteride groups showed few fibrous connective tissues without white membrane structure. The urethral tissue in the finasteride groups was thin and relatively compact.

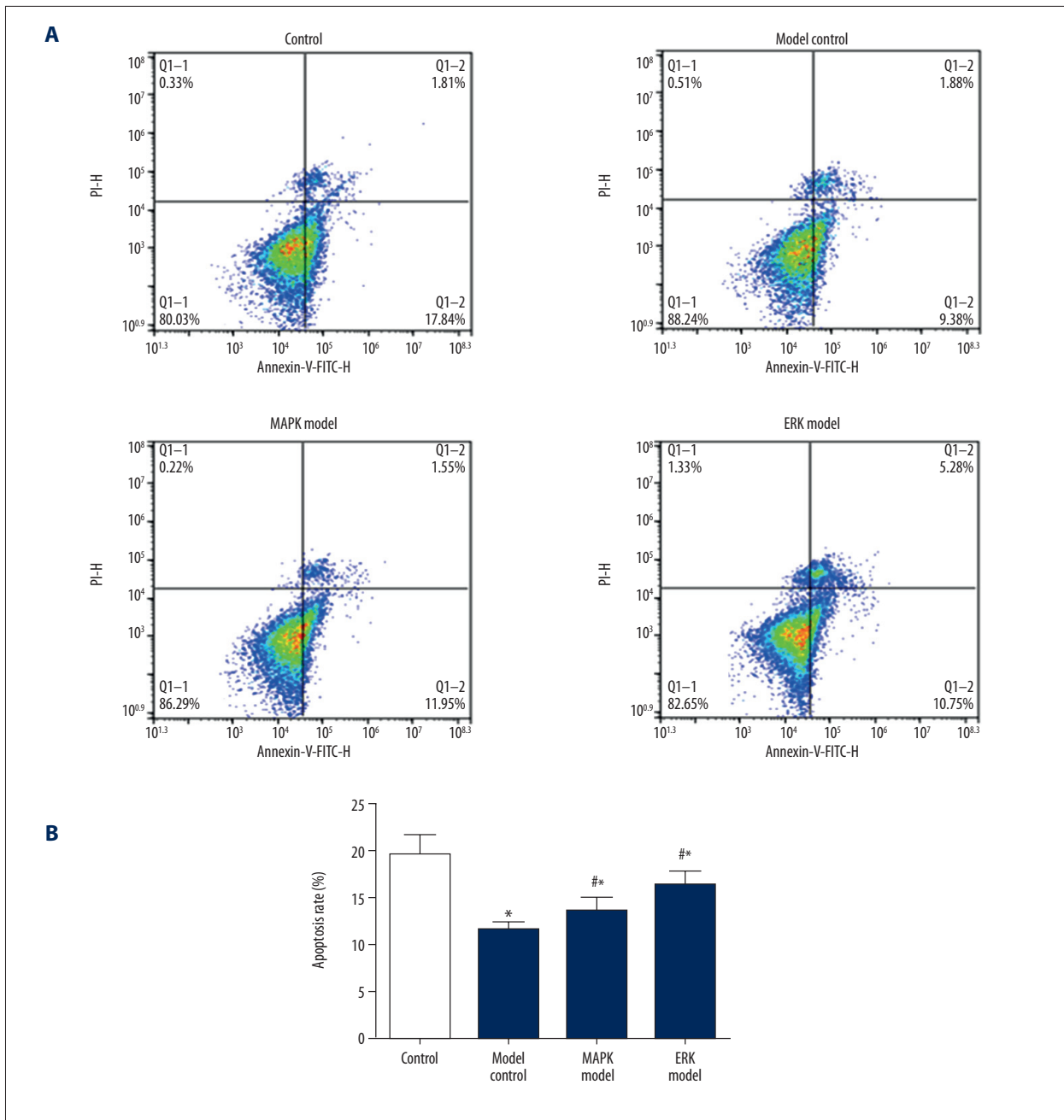


Figure 3. Apoptosis of urethral plate fibroblasts was enhanced by MAPK inhibitor or ERK inhibitor. **(A)** Representative image of flow cytometry. **(B)** Quantification data of the apoptosis. Compared with control, * $P < 0.05$; compared with model, # $P < 0.05$.

Proliferation of urethral plate fibroblasts was attenuated by MAPK inhibitor or ERK inhibitor

The UPF were identified by immunofluorescence. As shown in Figure 2A, the red staining shows the target protein and the blue staining is the nucleus. The results showed that most of the cells expressed Vimentin specifically, which proved that the UPF were successfully separated.

Proliferation of UPF in the model group was higher than that of the control group (Figure 2B), and the difference was statistically significant ($P < 0.05$). Compared with the model group, MAPK inhibitor or ERK inhibitor significantly reduced the cell proliferation, and the difference was statistically significant ($P < 0.05$). By contrast, there was no statistically significant difference between the ERK inhibitor and MAPK inhibitor groups ($P > 0.05$).

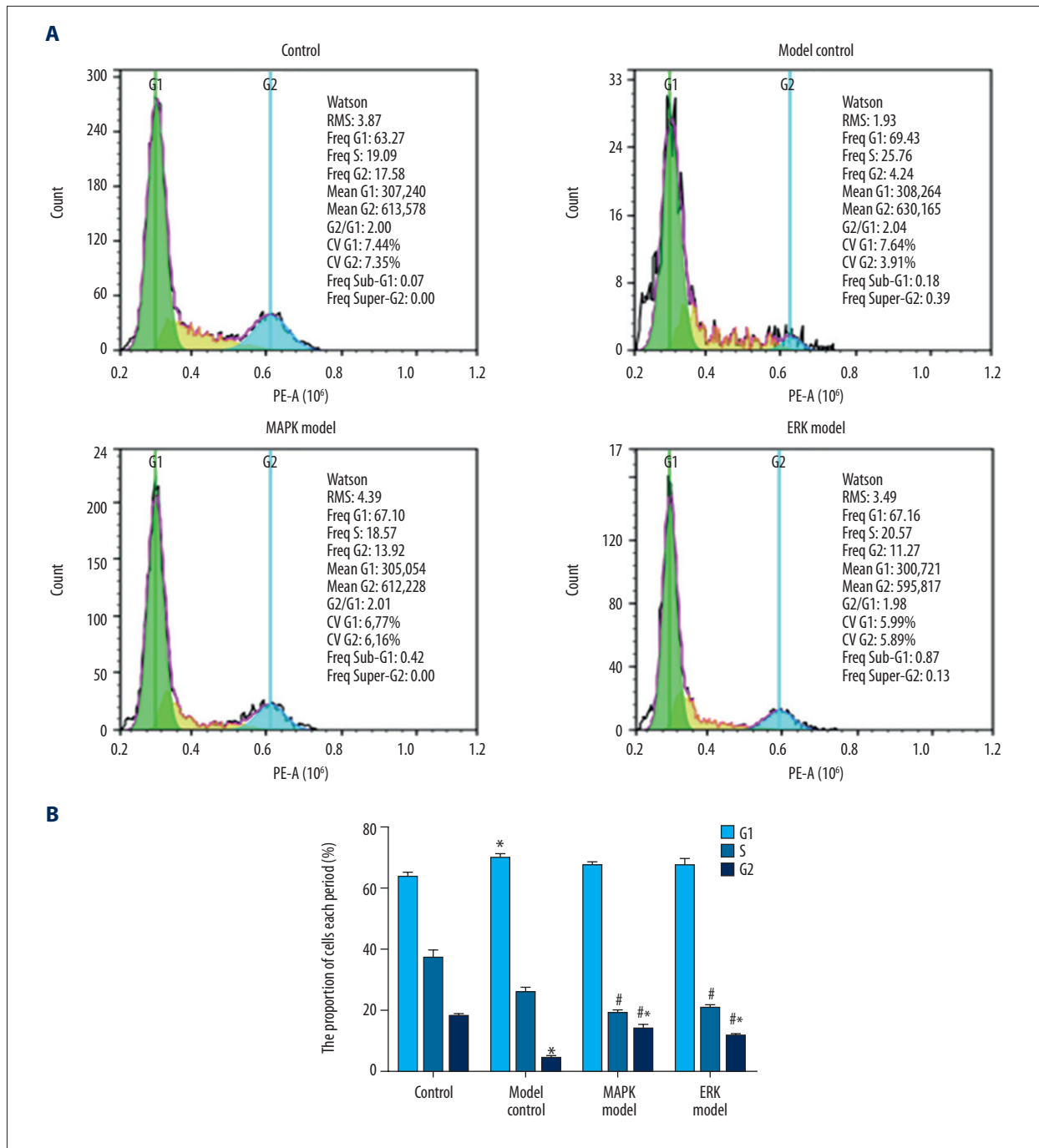


Figure 4. Cell cycling of urethral plate fibroblasts was attenuated by MAPK inhibitor or ERK inhibitor. **(A)** Representative image of flow cytometry. **(B)** Quantification data of the cell numbers in G1, S, G2 phases. Compared with control, * $P < 0.05$; compared with model, # $P < 0.05$.

Apoptosis of urethral plate fibroblasts was enhanced by MAPK inhibitor or ERK inhibitor

Compared with the normal control group, the model group showed lower apoptotic rate, and the difference was statistically significant ($P < 0.05$) (Figure 3). Compared with the model

group, apoptotic rates in the MAPK inhibitor group and ERK inhibitor group were higher, and the difference was statistically significant ($P < 0.05$). Among them, the apoptotic rate of ERK inhibitor group was the highest, and the difference was statistically significant (vs. MAPK, $P < 0.05$).

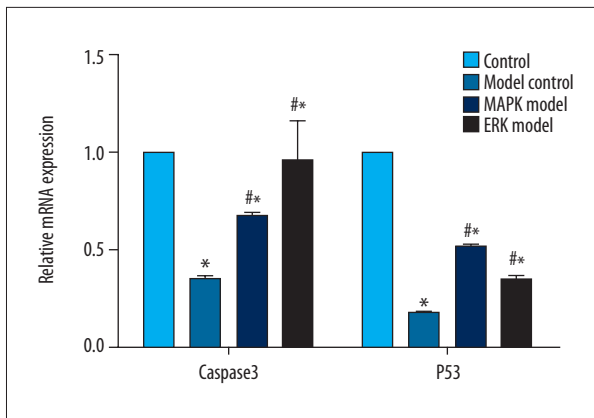


Figure 5. Caspase-3 and P53 expression at mRNA level was enhanced by MAPK inhibitor or ERK inhibitor. Compared with control, * $P < 0.05$; compared with model, # $P < 0.05$.

Cell cycling of urethral plate fibroblasts was attenuated by MAPK inhibitor or ERK inhibitor

Compared with the control group, the cell numbers in G1 and S phases in the model group was higher, while cell numbers in G2 phase were lower ($P < 0.05$) (Figure 4). By contrast, MAPK inhibitor or ERK inhibitor attenuated the abnormal cell cycle distribution (vs. model, $P < 0.05$). There was no significant difference between the ERK inhibitor group and MAPK inhibitor group ($P > 0.05$).

Apoptosis-related gene expression was enhanced by MAPK inhibitor or ERK inhibitor

As compared with the control group, the expression of caspase 3 and P53 at mRNA level in the cells of the model group was significantly reduced. By contrast, MAPK inhibitor and ERK inhibitor significantly attenuated the effect of finasteride ($P < 0.05$). Caspase 3 and P53 in the MAPK inhibitor and ERK inhibitor groups were comparable (Figure 5).

Compared with the control group, the expression of p-MAPK14/MAPK14 in the model group was promoted. By contrast, a MAPK inhibitor and an ERK inhibitor significantly reduced P-MAPK14/MAPK14 (vs. model, $P < 0.05$). The expression of p-MEK1/MEK1, caspase 3, and P53 were reduced in the model group but were promoted in the MAPK inhibitor and ERK inhibitor groups (Figure 6).

Discussion

Hypospadias is a congenital malformation of the urethral tissue, while finasteride is recognized as a drug that can induce hypospadias in male embryos. The effect is mainly by blocking the conversion of testosterone to DHT and reducing the DHT level. Through screening different doses of finasteride, hypospadias was also identified by HE staining. We found that the heterotopic urethral cavernosum was abundant when the dose of finasteride was 10 mg/kg, which indicated that the animal model of congenital hypospadias was successfully established. After that, the UPF were obtained from normal

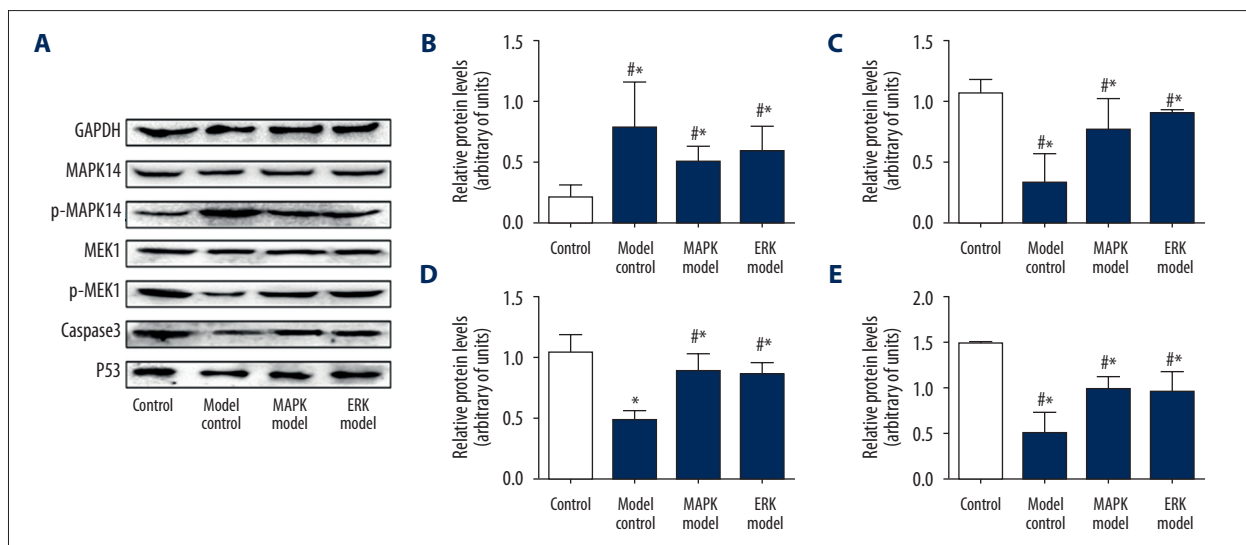


Figure 6. Apoptosis-related gene expression was enhanced by MAPK inhibitor or ERK inhibitor. (A) Representative blots of caspase-3, P53, p-MAPK14, and p-MEK. (B) Quantification data of p-MAPK14/MAPK14; (C) Quantification data of p-MEK1/MEK1; (D) Quantification data of caspase 3; (E) Quantification data of P53. Compared with control, * $P < 0.05$; compared with model, # $P < 0.05$.

control and modeled rats, and the results of immunofluorescence showed that most of the cells expressed vimentin specifically, which proved that UPF were successfully collected.

Activation of the MAPK/ERK signaling pathway can promote gene expression and change the cellular physiological activities, including differentiation and apoptosis [20,21]. In the present study, the proliferation and apoptosis of UPF was detected after treatment of a MAPK inhibitor and an ERK inhibitor, respectively. We found that the proliferation was promoted in UPF obtained from modeled rats, which supports that uncontrolled proliferation of urethral plate fibroblasts might be an important cause of hypospadias [22,23]. To verify the results of proliferation, flow cytometry was used to detect apoptosis of the UPF in each group. Interestingly, apoptosis was reduced in the UPF obtained from modeled rats. Besides the reduced apoptosis, the cell cycling of UPF was also detected. Our results demonstrated that the cells in G1 and S phases were enhanced in the model group. Collectively, the proliferation activity of the UPF in the hypospadias group was higher than that in the normal control group, which might be caused by reduction of apoptosis and change of cell cycle. Importantly, the MAPK inhibitor and the ERK inhibitor effectively inhibited the proliferation of UPF. Moreover, apoptosis was promoted after MAPK and ERK inhibitor treatment. These results suggest that hypospadias has a relationship with the MAPK/ERK signaling pathway, which may be caused by the inhibition of cell apoptosis and enhanced cell cycling.

Apoptosis is the main form of programmed cell death in normal physiological states, and there is an important relationship between apoptosis and normal development of the urethra system. Abnormal apoptosis may lead to abnormal development of the urethral system [24]. The MAPK/ERK signaling pathway is involved in the processes of cell differentiation, proliferation, development, and apoptosis [25–27]. In the present study, the expression of P-MAPK14/MAPK14 and p-MEK1/MEK1 was detected, and the results demonstrated that the relative expression of P-MAPK14/MAPK14 in the cells of the model group was upregulated, while the amount of p-MEK1/MEK1 expression decreased simultaneously compared with the control group. In contrast, the relative expression of P-MAPK14/MAPK14 in the MAPK inhibitor group and the ERK inhibitor group was

reduced accordingly, while the p-MEK1/MEK1 expression increased. These results suggest that apoptosis of UPF in the hypospadias group is related to the level of P-MAPK14/MAPK14 and p-MEK1/MEK1, and show that apoptosis can be promoted by downregulation of MAPK14 and upregulation of MEK1.

Caspase 3 belongs to a class of specific proteolytic enzymes in the caspase family and is one of the most important effectors of apoptosis [28,29]. Caspase in the cytoplasm receives the apoptosis signal only when cells undergo apoptosis, and caspase activates inactive zymogen to active caspases [30,31]. In the present study, the expression of caspase 3 in each group of UPF was detected. The results showed that the expression of caspase 3 in the model group was reduced, while the MAPK inhibitor and the ERK inhibitor significantly upregulated the caspase 3 expression. These results reveal that the MAPK signaling pathway is related to apoptosis of UPF through regulating expression of caspase 3.

P53 is an important cyclin regulatory factor that mainly participates in cell proliferation by regulating G1 and S phases [32]. In the present study, the expression of P53 of UPF was detected. The results showed that the expression of P53 in the model group was reduced, while the MAPK inhibitor and the ERK inhibitor significantly upregulated P53 expression. These results suggest that inhibition of the expression of MAPK or ERK affects apoptosis. Based upon previous publications [33,34], the main downstream effectors of MAPK and ERK are different, in which caspase 3 is the main effective factor of MAPK, while P53 is the main effective factor of ERK. Based upon these data, MAPK/ERK could be a therapeutic target for the disease treatment, although *in vivo* evidence is still required.

Conclusions

Our study reveals that the MAPK/ERK signaling pathway is involved in the regulation of proliferation, apoptosis, and cell cycling of UPFs. Excessive proliferation of UPFs might cause obstruction of the urethra plate, resulting in hypospadias. Nevertheless, *in vivo* experiments are still needed to confirm our findings.

References:

1. Kim WJ, Hayashi C, Yamazaki Y: Age-related changes in urinary flow following dorsal inlay graft urethroplasty for hypospadias in early childhood: Potential improvement over 11 years of age. *J Pediatr Urol*, 2018; 14(3): 278.e1–278.e5
2. Thorup J, Nordenskjold A, Hutson JM: Genetic and environmental origins of hypospadias. *Curr Opin Endocrinol Diabetes Obes*, 2014; 21: 227–32
3. Gallentine ML, Morey AF, Thompson IM Jr.: Hypospadias: A contemporary epidemiologic assessment. *Urology*, 2001; 57: 788–90
4. Suzuki H, Matsushita S, Suzuki K, Yamada G: 5alpha-Dihydrotestosterone negatively regulates cell proliferation of the periurethral ventral mesenchyme during urethral tube formation in the murine male genital tubercle. *Andrology*, 2017; 5: 146–52
5. Qian C, Dang X, Wang X et al: Molecular mechanism of microRNA-200c regulating transforming growth factor-beta (TGF-beta)/SMAD family member 3 (SMAD3) pathway by targeting zinc finger E-box binding homeobox 1 (ZEB1) in hypospadias in rats. *Med Sci Monit*, 2016; 22: 4073–81

6. Kim EH, Brockman JA, Andriole GL: The use of 5-alpha reductase inhibitors in the treatment of benign prostatic hyperplasia. *Asian J Urol*, 2018; 5: 28–32
7. Fertig RM, Gamret AC, Darwin E, Gaudi S: Sexual side effects of 5-alpha-reductase inhibitors finasteride and dutasteride: A comprehensive review. *Dermatol Online J*, 2017; 23(11): pii: 13030/qt24k8q743
8. Lowe FC, McConnell JD, Hudson PB et al: Long-term 6-year experience with finasteride in patients with benign prostatic hyperplasia. *Urology*, 2003; 61: 791–96
9. Clark RL, Antonello JM, Grossman SJ et al: External genitalia abnormalities in male rats exposed in utero to finasteride, a 5 alpha-reductase inhibitor. *Teratology*, 1990; 42: 91–100
10. Ross AE, Marchionni L, Phillips TM et al: Molecular effects of genistein on male urethral development. *J Urol*, 2011; 185: 1894–98
11. Lai MS, Cheng YS, Chen PR et al: Fibroblast growth factor 9 activates akt and MAPK pathways to stimulate steroidogenesis in mouse leydig cells. *PLoS One*, 2014; 9: e90243
12. Dai X, Song R, Xiong Y: The expression of ERK and JNK in patients with an endemic osteochondropathy, Kashin-Beck disease. *Exp Cell Res*, 2017; 359: 337–41
13. Wang C, Li Z, Shao F et al: High expression of Collagen Triple Helix Repeat Containing 1 (CTHRC1) facilitates progression of oesophageal squamous cell carcinoma through MAPK/MEK/ERK/FRA-1 activation. *J Exp Clin Cancer Res*, 2017; 36: 84
14. Tidyman WE, Rauen KA: The RASopathies: Developmental syndromes of Ras/MAPK pathway dysregulation. *Curr Opin Genet Dev*, 2009; 19: 230–36
15. Tanti JF, Jager J: Cellular mechanisms of insulin resistance: Role of stress-regulated serine kinases and insulin receptor substrates (IRS) serine phosphorylation. *Curr Opin Pharmacol*, 2009; 9: 753–62
16. Strittmatter F, Gratzke C, Walther S et al: Alpha1-adrenoceptor signaling in the human prostate involves regulation of p38 mitogen-activated protein kinase. *Urology*, 2011; 78: 969 e7–13
17. Liu Y, Li Y, Li N et al: TGF-β1 promotes scar fibroblasts proliferation and transdifferentiation via up-regulating MicroRNA-21. *Sci Rep*, 2016; 6: 32231
18. Camelliti P, Borg TK, Kohl P: Structural and functional characterisation of cardiac fibroblasts. *Cardiovasc Res*, 2005; 65: 40–51
19. Wu YG, Li SK, Xin ZC et al: [The establishment of hypospadias rat model and embryoteratogenic test of Atrazine]. *Zhonghua Zheng Xing Wai Ke Za Zhi*, 2007; 23(4): 340–43 [in Chinese]
20. Luo H, Yanagawa B, Zhang J et al: Coxsackievirus B3 replication is reduced by inhibition of the extracellular signal-regulated kinase (ERK) signaling pathway. *J Virol*, 2002; 76: 3365–73
21. Yao Z, Seger R: The ERK signaling cascade – views from different subcellular compartments. *BioFactors*, 2009; 35: 407–16
22. Lin J, Xie C, Chen R, Li D: [Effect of epidermal growth factor and testosterone on androgen receptor activation in urethral plate fibroblasts in hypospadias]. *Zhong Nan Da Xue Xue Bao Yi Xue Ban*, 2016; 41(5): 507–12 [in Chinese]
23. Morgan EA, Nguyen SB, Scott V, Stadler HS: Loss of Bmp7 and Fgf8 signaling in Hoxa13-mutant mice causes hypospadias. *Development*, 2003; 130: 3095–109
24. van der Werff JF, Nievelstein RA, Brands E et al: Normal development of the male anterior urethra. *Teratology*, 2000; 61: 172–83
25. Jazirehi AR, Bonavida B: Cellular and molecular signal transduction pathways modulated by rituximab (rituxan, anti-CD20 mAb) in non-Hodgkin's lymphoma: Implications in chemosensitization and therapeutic intervention. *Oncogene*, 2005; 24: 2121–43
26. Huh JE, Kang KS, Chae C et al: Roles of p38 and JNK mitogen-activated protein kinase pathways during cantharidin-induced apoptosis in U937 cells. *Biochem Pharmacol*, 2004; 67: 1811–18
27. Cano E, Mahadevan LC: Parallel signal processing among mammalian MAPKs. *Trends Biochem Sci*, 1995; 20: 117–22
28. Zhu G, Wang X, Wu S, Li Q: Involvement of activation of PI3K/Akt pathway in the protective effects of puerarin against MPP+-induced human neuroblastoma SH-SY5Y cell death. *Neurochem Int*, 2012; 60: 400–8
29. Tron VA, Trotter MJ, Tang L et al: p53-regulated apoptosis is differentiation dependent in ultraviolet B-irradiated mouse keratinocytes. *Am J Pathol*, 1998; 153: 579–85
30. Karki P, Lee J, Shin SY, Cho B, Park IS: Kinetic comparison of procaspase-3 and caspase-3. *Arch Biochem Biophys*, 2005; 442: 125–32
31. Roy S, Bayly CI, Gareau Y et al: Maintenance of caspase-3 proenzyme dormancy by an intrinsic “safety catch” regulatory tripeptide. *Proc Natl Acad Sci USA*, 2001; 98: 6132–37
32. Shetty P, Velusamy T, Bhandary YP et al: Urokinase expression by tumor suppressor protein p53: A novel role in mRNA turnover. *Am J Respir Cell Mol Biol*, 2008; 39: 364–72
33. Nagahara Y, Kawakami K, Sikandan A et al: Sphingoid base-upregulated caspase-14 expression involves MAPK. *Biol Pharm Bull*, 2018; 41: 743–48
34. Li Q, Lei Y, Du W: A novel target of p53, TCF21, Can Respond to Hypoxia by MAPK pathway inactivation in uterine corpus endometrial carcinoma. *DNA Cell Biol*, 2018; 37: 473–80